Article

Chemistry & Biology

XBP1s Links the Unfolded Protein Response to the Molecular Architecture of Mature N-Glycans

Graphical Abstract

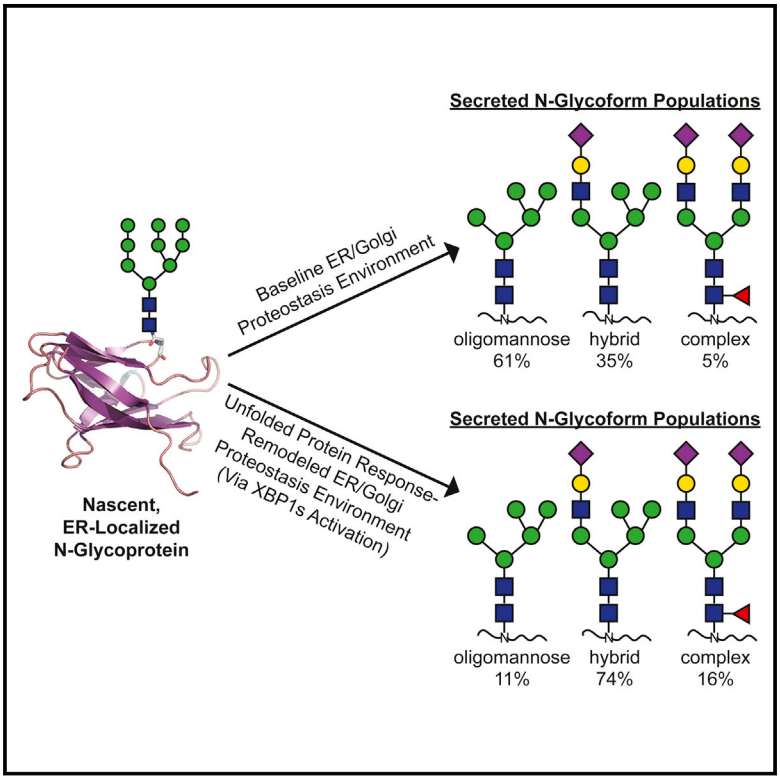

Highlights

- XBP1s regulates N-glycan maturation pathways, in addition to proteostasis
- XBP1s can enhance synthesis of hybrid and complex N-glycans on secreted proteins
- Regulating N-glycodynamics is a new function for the unfolded protein response
- XBP1s-mediated alterations in the N-glycome could have key biological impacts

Authors

Mahender B. Dewal, Andrew S. DiChiara, Aristotelis Antonopoulos, ..., Stuart M. Haslam, Anne Dell, Matthew D. Shoulders

Correspondence

mshoulde@mit.edu

In Brief

The molecular architecture of the N-glycome is regulated by poorly defined mechanisms. Dewal et al. now demonstrate that the unfolded protein response plays a critical role in N-glycan maturation, unveiling a functional link between intracellular proteostasis and extracellular N-glycoprotein structures.

Dewal et al., 2015, Chemistry & Biology *22*, 1301–1312
October 22, 2015
http://dx.doi.org/10.1016/j.chembiol.2015.09.006

Chemistry & Biology
Article

XBP1s Links the Unfolded Protein Response to the Molecular Architecture of Mature N-Glycans

Mahender B. Dewal,[1] Andrew S. DiChiara,[1] Aristotelis Antonopoulos,[2] Rebecca J. Taylor,[1] Chyleigh J. Harmon,[1] Stuart M. Haslam,[2] Anne Dell,[2] and Matthew D. Shoulders[1,*]
[1]Department of Chemistry, Massachusetts Institute of Technology, 77 Massachusetts Avenue, Cambridge, MA 02139, USA
[2]Department of Life Sciences, Imperial College London, London SW7 2AZ, UK
*Correspondence: mshoulde@mit.edu
http://dx.doi.org/10.1016/j.chembiol.2015.09.006

SUMMARY

The molecular architecture of the mature N-glycome is dynamic, with consequences for both normal and pathologic processes. Elucidating cellular mechanisms that modulate the N-linked glycome is, therefore, crucial. The unfolded protein response (UPR) is classically responsible for maintaining proteostasis in the secretory pathway by defining levels of chaperones and quality control proteins. Here, we employ chemical biology methods for UPR regulation to show that stress-independent activation of the UPR's XBP1s transcription factor also induces a panel of N-glycan maturation-related enzymes. The downstream consequence is a distinctive shift toward specific hybrid and complex N-glycans on N-glycoproteins produced from XBP1s-activated cells, which we characterize by mass spectrometry. Pulse-chase studies attribute this shift specifically to altered N-glycan processing, rather than to changes in degradation or secretion rates. Our findings implicate XBP1s in a new role for N-glycoprotein biosynthesis, unveiling an important link between intracellular stress responses and the molecular architecture of extracellular N-glycoproteins.

INTRODUCTION

The endoplasmic reticulum (ER) is a specialized protein-folding factory responsible for producing about one-third of the proteome (Braakman and Bulleid, 2011). The vast majority of proteins traversing the ER are co- or post-translationally N-glycosylated by oligosaccharyl transferase (OST) (Aebi, 2013; Zielinska et al., 2010). A 14-residue oligosaccharide with the structure $Glc_3Man_9GlcNAc_2$ is transferred by OST from the lipid-linked precursor $Glc_3Man_9GlcNAc_2$-pyrophosphate-dolichol to the amide nitrogen of Asn side chains in Asn-Xaa-Ser/Thr sequons (where Xaa ≠ Pro). This immature N-linked glycan is later processed and modified in both the ER and the Golgi to ultimately yield the vast array of distinct molecular structures observed on mature ER clients (Moremen et al., 2012).

Protein N-glycosylation has important implications for numerous normal and pathologic processes (Dennis et al., 2009), including protein folding and stability (Chen et al., 2010; Culyba et al., 2011), function (Venetz et al., 2015), trafficking (Wujek et al., 2004), quality control (Ruiz-Canada et al., 2009), and aggregation (Ioannou et al., 1998), as well as auto-immunity and tumor metastasis (Chui et al., 2001; Häuselmann and Borsig, 2014). Furthermore, although the architecture of the highly diverse, mature N-linked glycome is known to be dynamic, responding to environmental conditions and other stimuli (Hassinen et al., 2011; Lau et al., 2007), the upstream cellular mechanisms that regulate the composition of the N-glycome remain poorly delineated (Voss et al., 2014). Elucidating those mechanisms is important not just for understanding normal and disease physiology, but also for optimizing the production of recombinant proteins displaying desirable N-glycoform populations (Elliott et al., 2003).

The composition of the secretory pathway's proteostasis network, which is responsible for the folding and quality control of secreted, transmembrane, and lysosomal proteins, including all N-glycoproteins, is regulated by the unfolded protein response (UPR) (Ron and Walter, 2007). The UPR typically activates in response to ER stress caused by the accumulation of unfolded and misfolded proteins. Aside from transient inhibition of new protein synthesis, the crucial consequence of this stress-responsive UPR activation is a large-scale remodeling of the ER proteostasis network via transcriptional upregulation of chaperones, folding enzymes, and quality control factors. These transcriptional responses are propagated by two UPR-specific transcription factors, X-box binding protein 1-spliced (XBP1s) and activating transcription factor 6 (ATF6), as well as a third transcription factor, activating transcription factor 4, which can also be induced by independent stress response pathways (Schröder and Kaufman, 2005). UPR-mediated upregulation of chaperones and quality control mechanisms can restore ER proteostasis in response to a variety of protein misfolding-inducing stressors.

A classic method to activate the UPR and thereby study its function is the inhibition of ER client protein N-glycosylation by treatment with tunicamycin (Tm), which prevents the synthesis of the dolichol-linked N-glycan precursor (Lehle and Tanner, 1976), highlighting the importance of N-glycosylation for ER proteostasis. The absence of N-linked glycans on nascent ER clients prevents access to the key ER lectin-based chaperones calnexin and calreticulin, restricts monitoring by the lectin-based quality-control machinery, and can also intrinsically destabilize ER clients (Hammond et al., 1994).

Thus, the paradigmatic role of the UPR is to upregulate chaperones and quality-control mechanisms in response to protein

misfolding stress. Because N-glycosylation sequons are normally only partially occupied (Zielinska et al., 2010), it is reasonable to also expect that UPR activation might enhance the extent of ER client protein N-glycosylation (Hammond et al., 1994; Spear and Ng, 2005; Thibault et al., 2011). Such an enhancement would specifically increase access to lectin-based proteostasis mechanisms. Consistent with this concept, ER stress can upregulate hexosamine biosynthesis to promote ER client clearance and prolong life in the face of chronic protein misfolding stress (Denzel et al., 2014; Wang et al., 2014).

We speculated that the UPR might regulate not just the extent of protein N-glycosylation, but also the molecular structure of mature N-glycans. Mature N-glycan architectures are substantially altered in many malignancies (Fry et al., 2011; Häuselmann and Borsig, 2014; Stowell et al., 2015), yet the mechanisms that regulate these altered N-glycosylation patterns remain ill-defined. Concomitantly, it is intriguing to note that a number of malignancies appear to rely on the activation of pro-survival pathways within the UPR, including constitutive activation of the XBP1s transcription factor (Bagratuni et al., 2010; Carrasco et al., 2007; Fujimoto et al., 2003). These observations, in addition to the overarching role of the UPR in regulating ER client protein folding and trafficking, suggested to us that there may be a connection between UPR activity and N-glycan maturation patterns.

Testing our hypothesis requires studying the biosynthesis of N-glycoproteins in the presence or absence of UPR-mediated remodeling of the ER proteostasis network. Unfortunately, ER stress-inducing small molecules such as Tm, thapsigargin, or DTT activate the UPR by creating non-physiologic levels of protein misfolding stress and are highly cytotoxic. These undesired side effects convolute efforts to study the roles of UPR activation and the resultant ER proteostasis network remodeling in protein maturation.

To overcome this challenge, small molecule-regulated methods for the orthogonal, stress-independent activation of the key adaptive UPR transcription factors XBP1s and ATF6 in human cells have been pioneered (Lee et al., 2003; Shoulders et al., 2013b). Specifically, the ATF6 transcription factor can be regulated by fusion to a dihydrofolate reductase (DHFR) destabilized domain that is stabilized by administration of trimethoprim (TMP) (Iwamoto et al., 2010; Shoulders et al., 2013a), while XBP1s can be placed under control of the tetracycline repressor and activated by doxycycline (Dox). In cells carrying these chemical genetic tools, such as the HEK293^{DAX} cell line (Shoulders et al., 2013b), the functional consequences of physiologically relevant, UPR transcription factor-mediated remodeling of the ER proteostasis network can be studied in the absence of toxic protein misfolding stress created by molecules such as Tm, thapsigargin, or DTT.

Here, we employ stress-independent UPR activation to elucidate whether and how UPR-mediated remodeling of the ER proteostasis network regulates N-glycan maturation. We demonstrate that the XBP1s transcription factor is responsible for modulating N-glycan maturation on model secreted proteins, resulting in enhanced synthesis of both hybrid and complex N-glycans. Our observations indicate that the IRE1-XBP1s axis of the UPR can modify N-glycan maturation, unveiling a previously unknown link between intracellular proteostasis mechanisms and the molecular architecture of extracellular N-glycoproteins.

RESULTS

Transcriptional Regulation of N-Glycan Biosynthesis and Maturation Pathways by the Unfolded Protein Response

Affymetrix whole-genome arrays were previously used to evaluate the transcriptome of HEK293^{DAX} cells upon small-molecule-mediated activation of XBP1s and/or ATF6 (Shoulders et al., 2013b). It was observed that these transcription factors control the levels of partially overlapping sets of ER chaperoning and quality control mechanisms. Interestingly, gene ontology enrichment analysis shows that five of the top 24 and two of the top ten gene sets induced by XBP1s are related to N-glycosylation of ER clients (Shoulders et al., 2013b). Of particular note, numerous components of the N-glycoprotein biosynthesis machinery are upregulated by XBP1s or the combination of XBP1s and ATF6 activation (see Table S1 for quantitative data), including components of the oligosaccharyltransferase complex and enzymes involved in the synthesis of the dolichol-linked precursor to N-glycosylation (Figure 1A, regular italic typeface).

Considering the essential roles of N-glycans in providing access to the ER proteostasis network (Hammond et al., 1994), it is not surprising that enzymes involved in the extent to which ER clients are N-glycosylated are upregulated by the UPR transcription factors. Intriguingly, we also observe numerous enzymes likely involved in N-glycan maturation that are upregulated by XBP1s activation or the combination of both XBP1s and ATF6 activation (Figure 1A, bold italic typeface) (Shoulders et al., 2013b). The possible connection to ER proteostasis is arguably less apparent for these enzymes than for those involved in initial N-glycoprotein biosynthesis. However, the UPR plays a critical role not just in protein folding, but also in ER client trafficking and propagating intracellular stress signals to the extracellular milieu (Taylor and Dillin, 2013). Therefore, motivated by these transcript-level results, we proceeded to explore the possible functional consequences of XBP1s and/or ATF6 activation for the maturation of N-glycans installed on ER client proteins.

XBP1s Modulates N-Glycan Maturation on a Secreted N-Glycoprotein

We elected to employ the CD2 adhesion domain, a well-characterized ER client protein (Culyba et al., 2011), in our initial studies. The *Rattus norvegicus* CD2 variant employed, henceforth termed CD2, has the sequence $K_{61}I_{62}F_{63}A_{64}N_{65}G_{66}T_{67}$ at its single N-glycosylation sequon, an N-terminal preprotrypsin signal sequence, a hexahistidine tag for purification, and a FLAG tag for immunoblotting and immunoisolation (Figure 1B) (Murray et al., 2015). CD2 secreted from HEK293 cells displays two distinctive N-linked glycoform populations that are readily separated by SDS-PAGE analysis (Figure 1C). We confirmed that the two bands observed by immunoblotting of secreted CD2 (N-glycoforms A indicated by the black arrowhead and N-glycoforms B by the gray arrowhead in Figure 1C) separate based on their distinctive N-glycan states by showing that peptide-N-glycosidase F (PNGase F) digestion collapses both bands into a single, lower molecular weight, non-glycosylated band indicated by the white arrowhead.

To investigate the influence of XBP1s- and/or ATF6-mediated remodeling of the ER proteostasis network on CD2 N-glycan

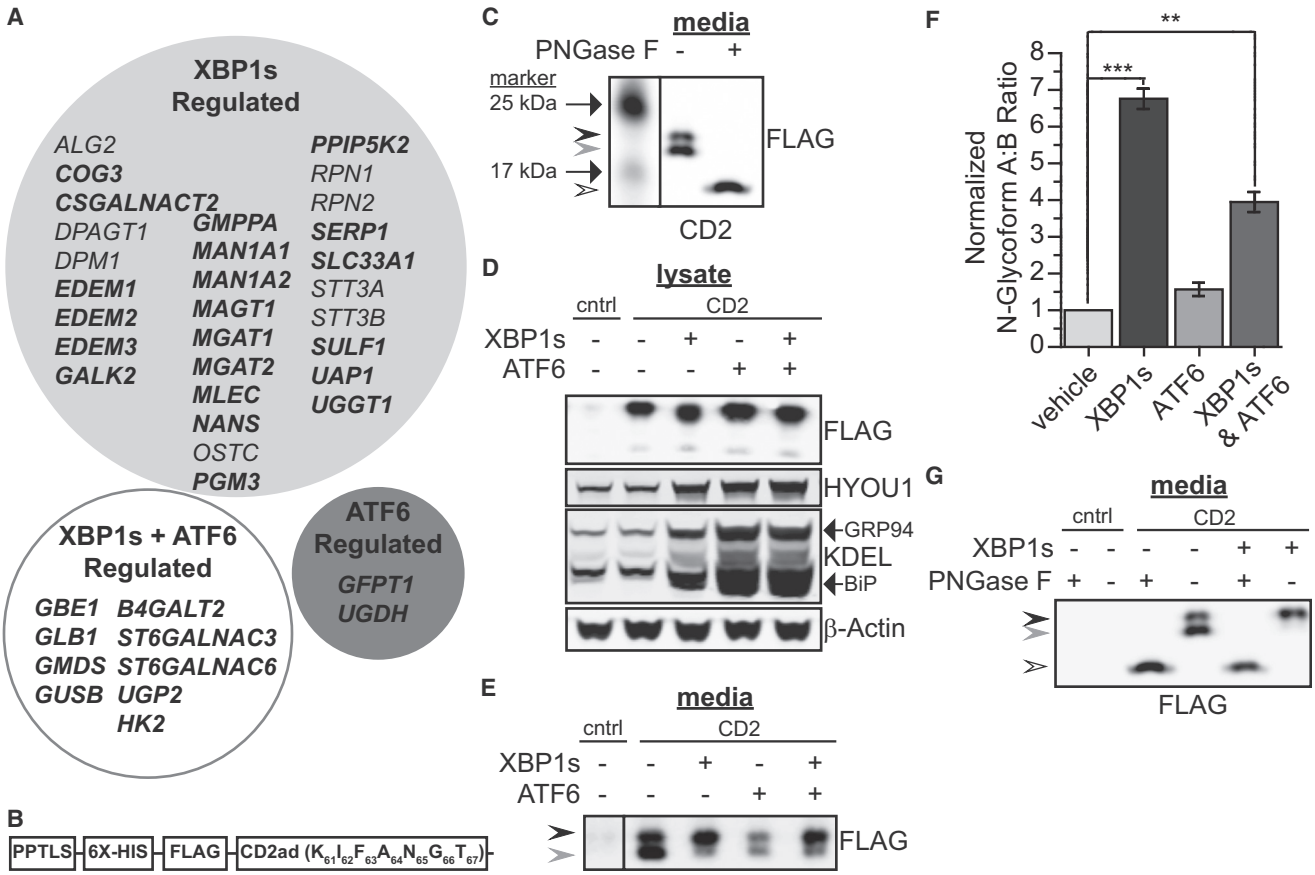

Figure 1. XBP1s Modulates the Molecular Architecture of CD2's N-Linked Glycan

(A) Gene ontology enrichment analysis identifies numerous genes involved in N-glycoprotein biosynthesis (regular italic typeface) and potentially in N-glycan maturation (bold italic typeface) that are upregulated primarily by XBP1s (light-gray circle). In addition, a subset of N-glycosylation-related genes is induced primarily by ATF6 (dark-gray circle) or only when both XBP1s and ATF6 are activated (white circle). *MGAT1* upregulation was identified by qPCR.

(B) The CD2 expression construct includes the preprotrypsin leader sequence (PPTLS), a 6x-His tag, a FLAG tag, and the single N-glycosylation sequon shown.

(C) Immunoblot of media harvested from HEK293 cells expressing CD2 displays two distinct bands; N-glycoforms A (black arrowhead) and N-glycoforms B (gray arrowhead). PNGase F digestion collapses both bands to a single lower molecular weight band (white arrowhead).

(D) Representative immunoblot of lysates from HEK293$^{DAX\text{-}CD2}$ cells after 72 hr of XBP1s and/or ATF6 activation (Dox at 1 μg/ml and/or TMP at 10 μM). A single N-glycosylated band and a faint non-N-glycosylated band are observed. Probing for known UPR-upregulated proteins confirms transcription factor activation.

(E) Representative immunoblot of CD2 in media corresponding to the lysate samples in (D). Control media is from parent HEK293^{DAX} cells.

(F) Quantification of the data in (E). Error bars represent SEM from biological replicates (n = 3). **p < 0.005, ***p < 0.0005.

(G) Immunoblot showing PNGase F digestion of CD2 secreted from HEK293$^{DAX\text{-}CD2}$ cells. N-Glycoforms A and B are indicated by the black and gray arrowheads, respectively, while the white arrowhead indicates the PNGase F-digested, non-N-glycosylated band.

See also Table S1 and Figure S1.

maturation, we used CD2-encoding lentivirus to generate stable, clonal HEK293^{DAX} cells constitutively expressing modest levels of CD2, which we termed HEK293$^{DAX\text{-}CD2}$ cells. The cells were treated with vehicle, 1 μg/ml Dox to activate XBP1s, 10 μM TMP to activate ATF6, or both Dox and TMP to activate both transcription factors. We confirmed successful activation of XBP1s and/or ATF6 by analysis of chaperones known to be induced by these transcription factors (Figure 1D) (Shoulders et al., 2013b), and ensured that global UPR activation does not occur upon Dox or TMP treatment by using qPCR to compare the effects of administering the ER stress-inducing small molecule thapsigargin (Figure S1A).

We next analyzed CD2 N-glycosylation in both the media and lysate samples by immunoblotting. In cell lysates, we observe a single high molecular weight N-glycosylated CD2 band and a low-intensity non-N-glycosylated CD2 band. Activation of XBP1s and/or ATF6 has no apparent impact on the intracellular quantity of CD2 or the extent of N-glycosylation (Figure 1D). Intriguingly, XBP1s and/or ATF6 activation do have distinctive impacts on secreted CD2 (Figure 1E). CD2 secreted from untreated cells displays the expected two N-glycoform bands in a nearly 1:1 ratio. A reduced quantity of CD2 is secreted upon ATF6 activation, but the ratio of N-glycoforms remains unchanged. The quantity of CD2 secreted upon XBP1s activation is similar to that in untreated cells. Most interestingly, upon XBP1s activation we observe a nearly complete shift of the CD2 N-glycoform population from N-glycoforms B (gray arrowhead) to N-glycoforms A (black arrowhead). Also intriguing, we

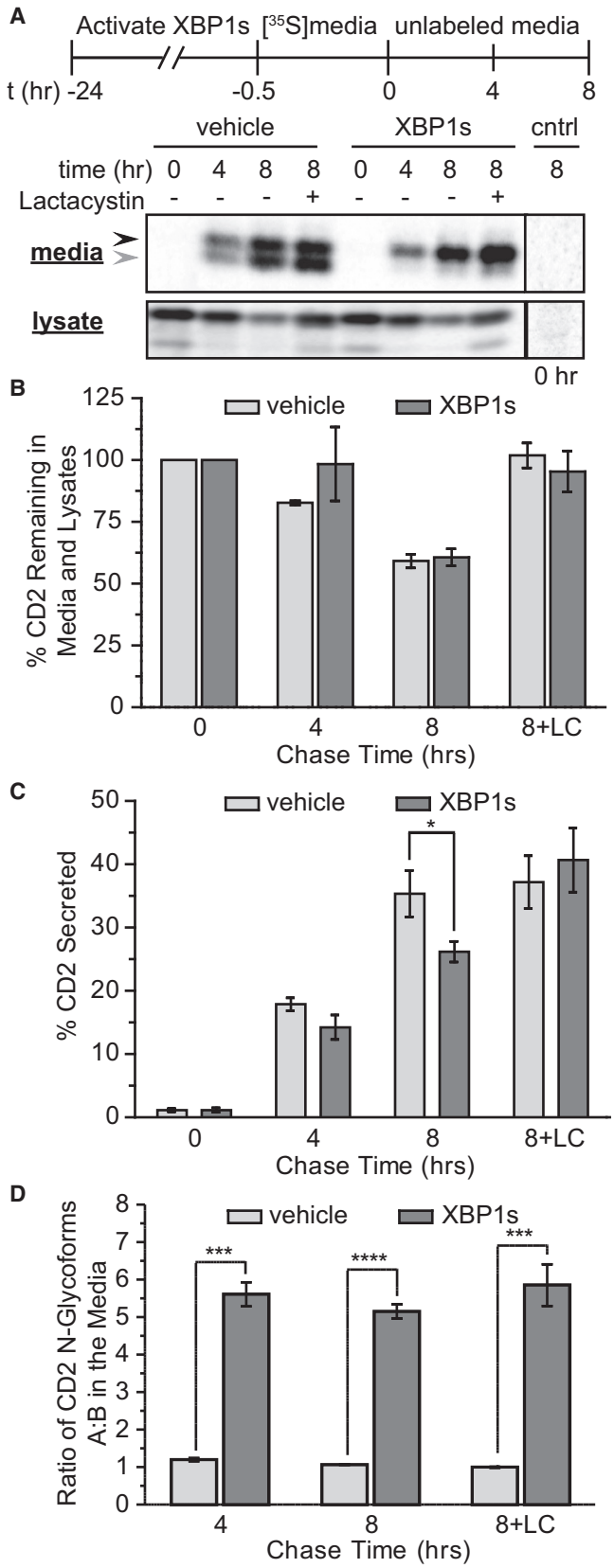

Figure 2. XBP1s Activation Does Not Significantly Influence CD2 Secretion or Degradation

(A) Representative auto-radiograms of ^{35}S-labeled CD2 immunoisolated from HEK293$^{DAX\text{-}CD2}$ media and lysates following a 24-hr pre-activation of XBP1s (Dox; 1 μg/ml) or no treatment. The metabolic labeling protocol employed is shown. Control media and lysate were harvested from parent HEK293^{DAX} cells. Lactacystin (LC) inhibits proteasomal degradation of CD2. Two N-glycoforms bands A and B are observed in the media, as indicated by the arrowheads.

(B–D) Quantification of auto-radiograms in (A). Percentage of CD2 remaining (B) was calculated by normalizing the secreted and lysate CD2 signal at the stated times to the total amount of labeled CD2 observed at time = 0 hr. Percentage of CD2 secreted (C) was calculated by normalizing the secreted CD2 signal to the total amount of CD2 present at time = 0 hr. The N-glycoforms ratio A/B (D) was calculated as in Figure 1F. Error bars represent SEM from biological replicates (n = 3). *p < 0.05, ***p < 0.005, ****p < 0.001.

observe the additive effect of XBP1s and ATF6 activation (B→A N-glycoforms shift and reduced secretion) when XBP1s and ATF6 are activated simultaneously.

Quantitation of the N-glycoform A/B ratio in XBP1s and vehicle-treated samples shows a highly significant, ~700% increase in the relative intensity of N-glycoforms A upon XBP1s activation relative to vehicle treatment (Figure 1F). PNGase F digestion of CD2 secreted from XBP1s-activated and untreated cells confirms that the shift in N-glycoform bands is attributable entirely to altered N-glycosylation, as opposed to other possible post-translational modifications (Figure 1G).

As a control, we analyzed CD2 in the media and lysates of transiently transfected HEK293^{DYG} cells (Shoulders et al., 2013b). In HEK293^{DYG} cells, TMP treatment stabilizes DHFR.YFP and Dox treatment induces eGFP. Analysis of CD2 in the media and lysates of HEK293^{DYG} cells shows no change in the extent of secretion or the N-glycoforms A/B ratio upon Dox and/or TMP treatment (Figures S1B and S1C). Thus, the results we observe in HEK293^{DAX} cells are attributable entirely to UPR transcription factor activation, not to any possible off-target effects of the small molecules employed.

In summary, XBP1s activation increases the levels of particular secreted CD2 N-glycoforms, while ATF6 activation has no apparent effect on the N-glycoforms but does reduce the extent of CD2 secretion. Because we were specifically interested in effects of the UPR on the molecular architecture of the mature N-glycome, we focused exclusively on CD2 produced from XBP1s-activated cells for further studies.

N-Glycoform Maturation Effects Mediated by XBP1s Activation Are Not Attributable to Altered Degradation or Secretion

The XBP1s-mediated shift in the N-glycoform population of mature, secreted CD2 could be caused by altered biosynthesis of the mature N-glycan in the Golgi. A more trivial explanation is that, under XBP1s-activated conditions, a particular CD2 N-glycoform is either degraded or secreted at a rate different to that in untreated cells. To test the latter hypothesis, we examined CD2's secretion and degradation rates in untreated and XBP1s-activated HEK293$^{DAX\text{-}CD2}$ cells using [^{35}S] metabolic labeling (Figure 2A). Relative to untreated cells, we found that XBP1s activation has no effect on the extent of CD2 degradation (Figure 2B). CD2 is indeed partially degraded by the proteasome,

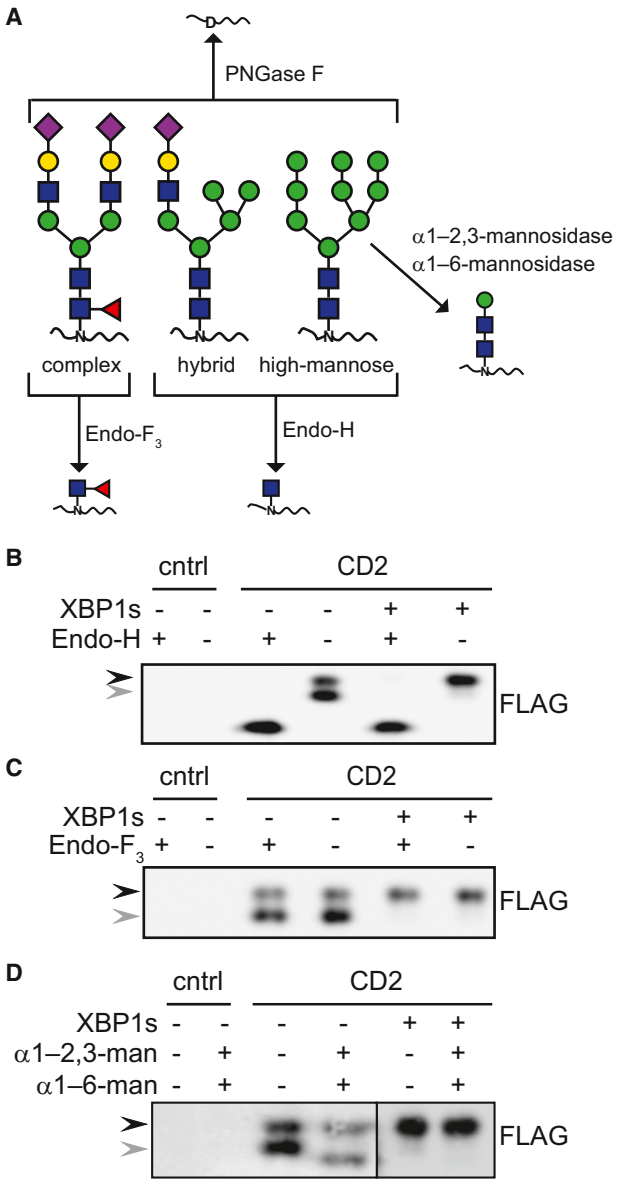

Figure 3. Glycosidase Digestions to Characterize N-Glycans on Secreted CD2

(A) Schematic displaying cleavage patterns of N-glycans by endo- and exo-glycosidases. Color symbols are: purple diamond, N-acetylneuraminic acid; blue square, N-acetylglucosamine; green circle, mannose; red triangle, fucose.

(B–D) Immunoblots of CD2 secreted from either untreated or XBP1s-activated HEK293$^{DAX-CD2}$ cells as in Figure 1E and digested with the indicated glycosidases. Endo-H cleaves both N-glycoforms A and B indicated by the black and gray arrowheads, yielding a mono-GlcNAcylated product (B). Endo-F_3 does not significantly cleave either N-glycoforms band (C). Double digestion by the α1–2,3- and α1–6-mannosidases reduces only the molecular weight of N-glycoforms B (D).

as shown by lactacystin-mediated proteasomal inhibition, but to a very similar overall extent under both sets of conditions. XBP1s activation may very modestly decrease the net secretion rate of CD2 over the course of 8 hrs ($p = 0.03$), but lactacystin treatment completely restores secretion to the levels of untreated cells (Figure 2C). Most importantly, at any time point in the pulse-chase experiment, and with or without proteasome inhibition, we observe the identical shift in the CD2 N-glycoforms ratio upon XBP1s activation (Figure 2D). These results demonstrate that the XBP1s-mediated effects on the architecture of the CD2 N-glycan cannot be attributed to altered CD2 secretion or degradation upon XBP1s activation.

XBP1s Activation Primarily Favors the Synthesis of Hybrid CD2 N-Glycans

To better understand how XBP1s activation alters N-glycan maturation, we next employed selective endo- and exo-glycosidase digestions to structurally classify the N-glycoforms A and B produced from both untreated and XBP1s-activated HEK293$^{DAX-CD2}$ cells. As illustrated in Figure 3A, Endo-H cleaves both high-mannose and hybrid N-glycans, Endo-F_3 cleaves only complex N-glycans, and the combination of α1–2,3-mannosidase and α1–6-mannosidase cleaves only high-mannose N-glycans (Jacob and Scudder, 1994). We found that Endo-H digests both CD2 N-glycoform bands A and B (at the sensitivity of an immunoblot), regardless of XBP1s activation (Figure 3B, black and gray arrowheads), suggesting that the majority of the CD2 N-glycans present are high-mannose or hybrid. Consistent with this observation, Endo-F_3 is unable to digest either CD2 N-glycoform band to an observable extent (Figure 3C). The combination of α1–2,3-mannosidase and α1–6-mannosidase, however, clearly reduces the molecular weight of N-glycoforms B (gray arrowhead), with no effect on N-glycoforms A (Figure 3D, black arrowhead). These observations suggest that XBP1s activation primarily enhances the biosynthesis of hybrid N-glycans on CD2.

Small Molecule-Mediated Inhibition of Mannosidases to Elucidate XBP1s-Mediated Effects on N-Glycan Biosynthesis

Following the transfer of the original 14-member, dolichol-linked N-glycan onto nascent ER client proteins, subsequent removal of the terminal glucose residues by the ER α-glucosidases I and II allows entry to the calnexin and/or calreticulin chaperone folding cycles (Caramelo and Parodi, 2008; Hammond et al., 1994). After folding, additional glucose and mannose residues are removed to yield high-mannose N-glycans that are then further digested by the Golgi α1–2-mannosidases (Herscovics, 1999). Subsequent to these mannosidase digestions, which yield various additional forms of high-mannose N-glycans, the N-glycan enters downstream processing into mature hybrid and complex N-glycans.

Our data from enzyme digestions indicate that the CD2 N-glycoforms band A, whose synthesis is strongly enhanced by XBP1s activation, is primarily hybrid. Therefore, we expected that inhibiting the catalytic activity of mannosidase I enzymes using kifunensine would eliminate the effects of XBP1s activation by preventing the production of mature high-mannose and hybrid N-glycans (Elbein et al., 1990). Indeed, we find that treatment with kifunensine results in observation of only a single N-glycoforms band for secreted CD2 (Figure 4A). Although this new band appears at a similar molecular weight to N-glycoforms band A in untreated cells, it is molecularly distinct. Unlike N-glycoforms band A (see Figure 3D), the single new band generated

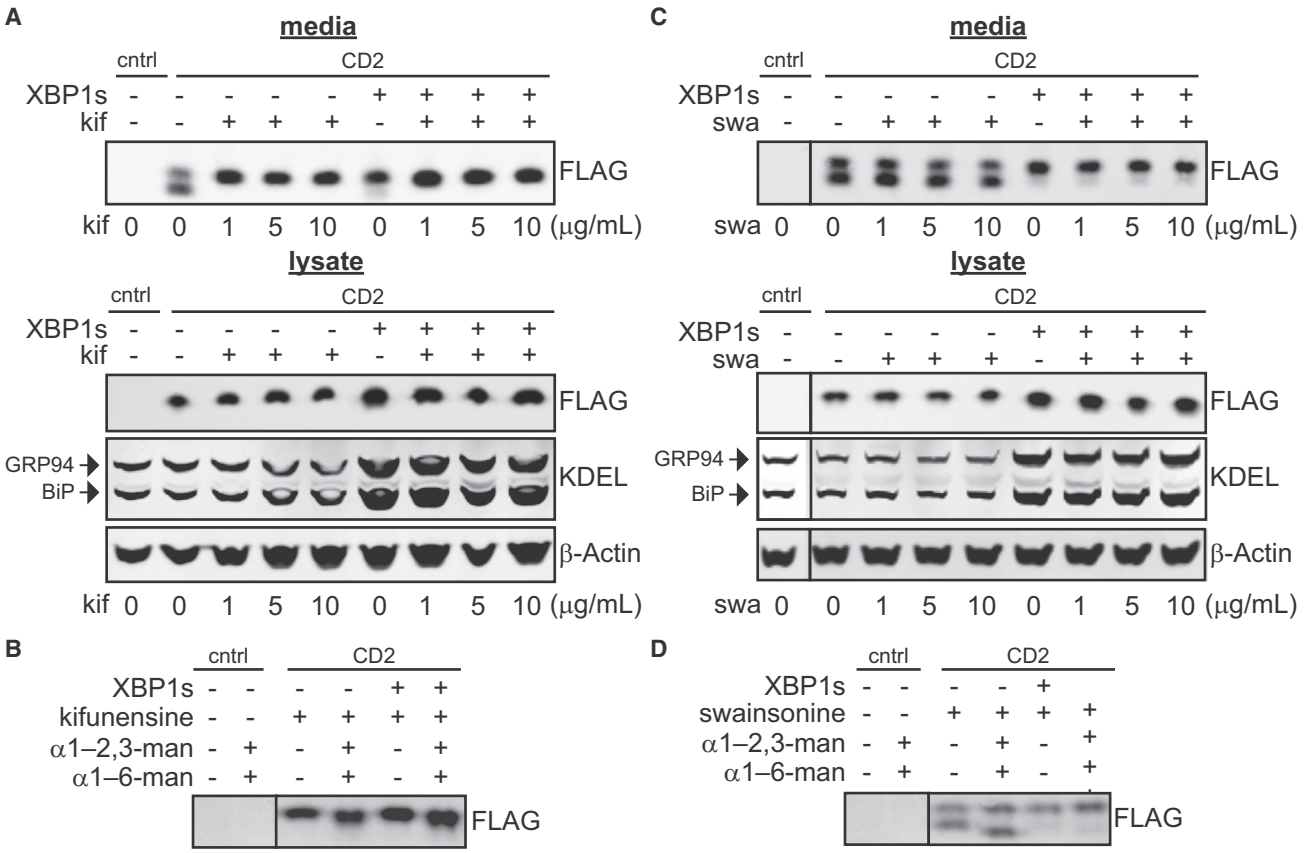

Figure 4. Effects of XBP1s Activation upon Inhibition of Mannosidases

Immunoblots are of CD2 secreted from untreated or XBP1s-activated HEK293$^{DAX\text{-}CD2}$ cells as in Figure 1E.

(A) Preventing formation of both hybrid and complex N-glycans by inhibiting mannosidases with kifunensine (kif) eliminates the effects of XBP1s activation on CD2 N-glycan maturation.

(B) Double digestion by the α1–2,3 -and α1–6-mannosidases reduces the molecular weight of secreted CD2 from (A), confirming that it is a high-mannose N-glycoform.

(C) Preventing formation of complex N-glycans by inhibiting α-mannosidase II with swainsonine (swa) has no observable impact on the effects of XBP1s activation on CD2 N-glycan biosynthesis.

(D) Double digestion by the α1–2,3- and α1–6-mannosidases only influences the molecular weight of N-glycoforms band B from non-XBP1s-activated HEK293$^{DAX\text{-}CD2}$ cells treated with swainsonine in (C).

See also Figure S2.

by kifunensine treatment is sensitive to digestion by α1–2,3-mannosidase and α1–6-mannosidase, as determined by the small but highly reproducible shift observable by immunoblotting that is expected for this digestion of a high-mannose N-glycoform (Figure 4B). Thus, these data show that the effects of XBP1s activation on N-glycan biosynthesis lie either at or downstream of the ER and Golgi mannosidase I enzymes.

Swainsonine inhibits Golgi α-mannosidase II (Tulsiani et al., 1982), which catalyzes a required step for complex N-glycan biosynthesis. Consistent with our enzyme digestions (Figure 3), swainsonine treatment has no observable impact on the N-glycoforms shift we detect upon XBP1s activation by immunoblotting (Figures 4C and 4D), suggesting once again that XBP1s is primarily enhancing the production of hybrid N-glycans on secreted CD2. We confirmed that Golgi α-mannosidase II is inhibited at the 10 μg/ml swainsonine concentration employed by demonstrating that this treatment prevents the formation of complex N-glycans on erythropoietin (Figure S2).

Glycomic Analysis of Purified CD2 by MALDI-TOF MS/MS

The data from our glycosidase digestion and inhibition studies suggest that XBP1s activation primarily increases hybrid N-glycan biosynthesis on CD2, at least at the resolution of a gel-based analysis. To obtain a molecular-level, more quantitative view of the effects of XBP1s on N-glycan maturation, we performed structural analysis on the N-glycans released from purified CD2 using MALDI-TOF tandem mass spectrometry (MS/MS) (Ceroni et al., 2008; Jang-Lee et al., 2006). We first optimized a protocol to obtain hundreds of μg quantities of highly purified secreted CD2 from both untreated and XBP1s-activated HEK293$^{DAX\text{-}CD2}$ cells (see Figure S3A). For the untreated sample, we separately extracted N-glycoforms bands A and B for MALDI-TOF MS/MS analysis. The N-glycoforms band B in the untreated sample (Figure 5A) is relatively homogeneous, with ~95% of the N-glycans being high-mannose and the ~5% hybrid likely deriving from cross-contamination by the higher

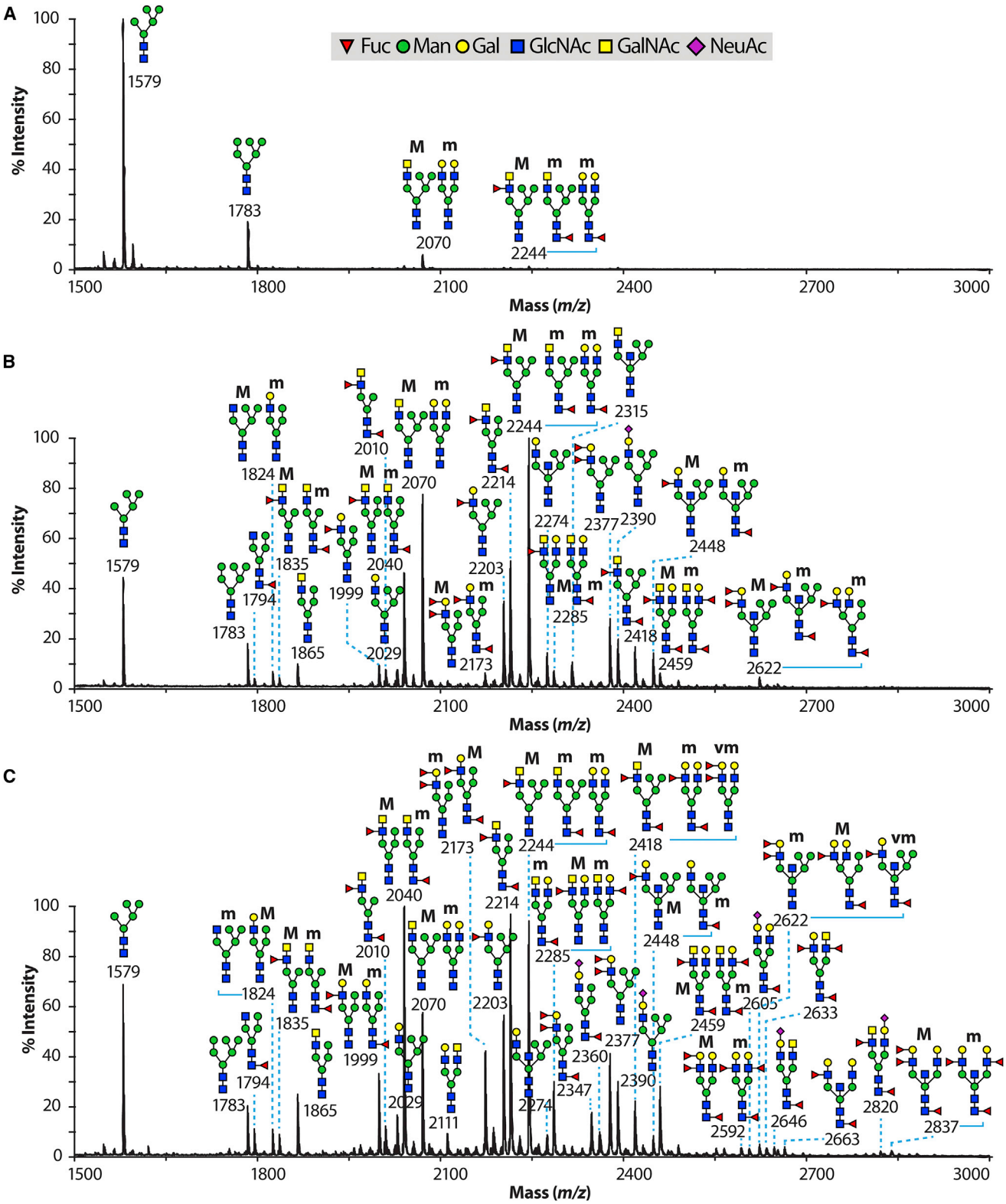

Figure 5. Mass Spectrometry-Based Glycomic Analyses Reveal the Molecular Structures of CD2 N-Glycans upon XBP1s Activation

MALDI-TOF mass spectra of permethylated N-glycans released by PNGase F digestion of CD2 purified from the media of untreated or XBP1s-activated HEK293$^{DAX\text{-}CD2}$ cells. In untreated cells, N-glycoforms bands A (A) and B (B) were analyzed separately. In XBP1s-activated cells, the bands were analyzed together (C).

(legend continued on next page)

Table 1. Summary of MALDI-TOF MS/MS Glycomic Analyses of CD2

	Vehicle (%)	XBP1s (%)
N-Glycan Classification Type		
Complex	5	16
Hybrid	35	74
High-mannose	61	11
N-Glycan Terminal Epitope[a]		
LacdiNAc	29	19
Fuc-LacdiNAc	47	39
LacNAc	10	15
LeX/A (Lewis X/A)[b]	4	10
LeY/B (Lewis Y/A)[b]	7	11
S-LacNAc[c]	4	6

[a]LacNAc, N-acetyllactosamine; LacdiNAc, N,N′-diacetyllactosamine; Fuc-LacdiNAc, fucosylated LacdiNAc; S-LacNAc, sialylated LacNAc.
[b]Lewis glycan epitope types.
[c]Sialylated LacdiNAc not detected.

molecular weight band A, owing to imperfect separation of the bands on SDS-PAGE. The N-glycoforms band A in the untreated sample is ~78% hybrid and ~9% complex (Figure 5B). After normalizing to the relative intensities of N-glycoforms bands A and B in untreated samples (Figure 1F), these MS results indicate that, in untreated cells, approximately 61% of the CD2 produced displays high-mannose N-glycans, ~35% hybrid, and ~5% complex (Table 1).

XBP1s activation almost entirely eliminates the lower molecular weight N-glycoforms band B, rendering separate extraction and glycomic analysis of N-glycoforms band B unfeasible. Therefore, for analysis of N-glycans on CD2 secreted from XBP1s-activated cells, we simply extracted the entire CD2 region from an SDS-PAGE gel (see Figure S3A). Strikingly, MALDI-TOF MS/MS analysis shows that ~11% of the N-glycans on CD2 produced from XBP1s-activated cells are high-mannose, ~74% are hybrid, and ~16% are complex (Figure 5C; Table 1). Normalizing to the relative intensities of bands A and B for the vehicle-treated sample, these results confirm our prediction from enzyme digestions and small-molecule inhibition experiments that XBP1s activation strongly favors the biosynthesis of hybrid N-glycans on CD2.

qPCR analyses show that transcripts for *MAN1A1* and *MGAT1* (which encodes GNT-I) are upregulated by XBP1s activation (Figure S3B). These two proteins are responsible for trimming mannose residues and transferring the first N-acetylglucosamine onto an N-glycan, two critical biosynthetic steps for formation of hybrid N-glycans, and thus could be involved in the observed XBP1s-mediated shift toward hybrid N-glycans. The higher sensitivity of the MALDI-TOF MS/MS analysis relative to immunoblotting allows us to also observe the >3-fold enhancement in the synthesis of complex N-glycans upon XBP1s activation, which could be mediated in part by MGAT2 (which encodes GNT-II), another protein whose transcript levels are upregulated by XBP1s (see qPCR data in Figure S3B). MGAT2 catalyzes an early step in the biosynthesis of complex N-glycans.

We note that a number of N-glycoforms are observed upon XBP1s activation that are simply not present on CD2 secreted from untreated cells (Figure 5). In addition, our MALDI-TOF MS/MS glycomic analyses provide molecular details regarding the terminal structures of the hybrid and complex N-glycans produced in untreated and XBP1s-activated cells. Of particular note, XBP1s activation shifts the population of terminal N-glycoform epitopes observed. Under untreated conditions, ~76% of the N-glycoforms display either LacdiNAc or Fuc-LacdiNAc terminal epitopes. Upon XBP1s activation this population drops to ~58%, with a corresponding modest increase in LacNAc, LeX/A, LeY/B, and sialylated (S-LacNAc) terminal epitopes (Table 1).

XBP1s-Mediated Effects on N-Glycan Maturation Are Generalizable beyond CD2 and HEK293 Cells

We wondered whether the effects on N-glycan biosynthesis we observe are CD2-specific, or are present more broadly for other N-glycoproteins. To explore this possibility, we created a construct for the expression and analysis of the collagen-α1(I) C-propeptide domain (Shoulders and Raines, 2009). We selected the collagen-α1(I) C-propeptide to study because, like CD2, this ~35-kDa secreted protein has a single N-glycosylation sequon and displays two N-glycoforms bands separable by SDS-PAGE upon secretion from HEK293^{DAX} cells. We analyzed hemagglutinin (HA) epitope-tagged collagen-α1(I) C-propeptide samples secreted from untreated and XBP1s-activated samples by immunoblotting. We observe that XBP1s activation once again increases the population of a higher molecular weight N-glycoforms band (Figures 6A and S4A), without altering the extent of protein secretion and with minimal effects on intracellular levels of the collagen-α1(I) C-propeptide (Figure 6B). Interestingly, ATF6 activation again decreases the net secretion of the protein with no apparent effects on N-glycosylation, while

(A) N-Glycoforms band B for CD2 secreted from untreated cells is homogeneous and high-mannose.
(B) N-Glycoforms band A for CD2 secreted from untreated cells is primarily hybrid.
(C) For CD2 from XBP1s-activated cells, N-glycoforms bands A and B were analyzed together. Hybrid and complex N-glycans are much more prominent in the XBP1s-activated sample than in the vehicle-treated sample (e.g., *m/z* 1,999, 2,040, 2,173, 2,214, 2,347, and 2,360 for hybrid structures and *m/z* 2,211, 2,285, 2,418, 2,459, 2,592, 2,605, 2,633, 2,646, 2,820, and 2,837 for complex structures), a difference whose magnitude is illustrated by normalizing to the relative intensities of bands A and B from vehicle-treated cells. Differences are also noted in the terminal N-glycan epitopes relative to untreated cells. These quantitations are presented in Table 1.
Color symbols are: yellow square, N-acetylgalactosamine; blue square, N-acetylglucosamine; yellow circle, galactose; green circle, mannose; purple diamond, N-acetylneuraminic acid; red triangle, fucose. All molecular ions are $[M + Na]^+$. Putative structures are based on composition, MS/MS, and biosynthetic knowledge. Structures that show sugars outside a bracket have not been unequivocally defined. Letters "vm", "m", and "M" in bold characters suggest very minor, minor, and major abundances, respectively.
See also Figure S3.

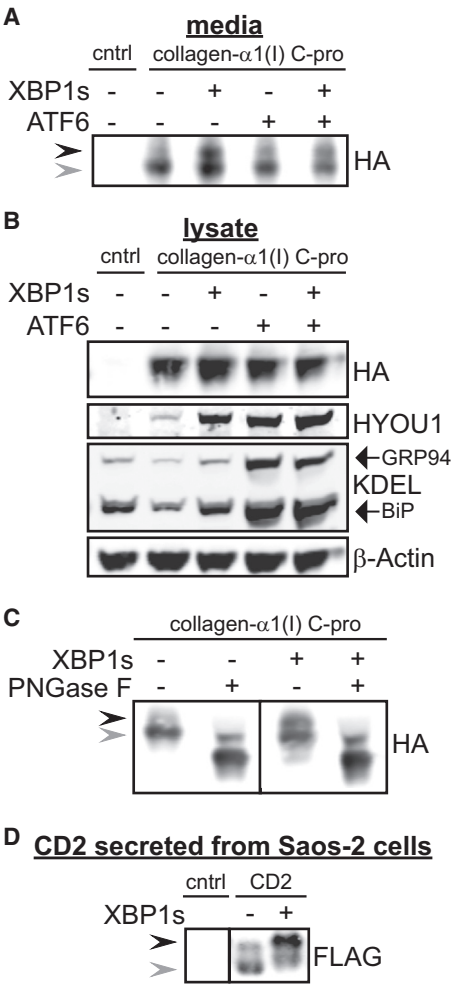

Figure 6. XBP1s Activation Modulates the Molecular Architecture of Mature N-Glycans on the Collagen-α1(I) C-Propeptide and in Saos-2 Cells

(A) Representative immunoblot of the collagen-α1(I) C-propeptide in media collected from HEK293^{DAX} cells stably expressing the protein after 48 hr of stress-independent XBP1s and/or ATF6 activation (Dox at 1 μg/ml and/or TMP at 10 μM). Two N-glycoforms bands A and B are observed, as indicated by the arrowheads. XBP1s activation enhances levels of the top band. Control media were harvested from parent HEK293^{DAX} cells.

(B) Representative immunoblot of lysates corresponding to the media samples in (A).

(C) Immunoblot showing PNGase F digestion of collagen-α1(I) C-propeptide samples secreted from untreated and XBP1s-activated HEK293^{DAX} cells as in (A). Two N-glycoforms bands A and B are observed, as indicated by the black and gray arrowheads, respectively.

(D) Immunoblot of CD2 secreted over 48 hr from transiently transfected Saos-2 cells co-transduced with either a GFP-encoding or an XBP1s-encoding adenovirus. Samples for analysis were obtained via a FLAG-M2-mediated immunoprecipitation of CD2 from the media. Two N-glycoforms bands A and B are observed, as indicated by the arrowheads. XBP1s activation enhances levels of the top band. Control media were harvested from GFP-transfected Saos-2 cells. See also Figure S4.

the combination of XBP1s and ATF6 activation displays an additive effect similar to the consequences for CD2 (Figure 6A). PNGase F digestion confirms that the XBP1s-induced shift is caused by an alteration in the N-glycans, as the banding patterns for collagen-α1(I) C-propeptides secreted from both XBP1s-activated and untreated cells are identical upon PNGase F digestion (Figure 6C).

We next queried whether the effects of XBP1s activity on N-glycan maturation are limited only to HEK293 cells. CD2 secreted from transiently transfected Saos-2 osteosarcoma cells is observed as a smear of N-glycoforms concentrated in two bands, as confirmed by PNGase F digestion (Figure S4B). We transiently transfected CD2 into Saos-2 osteosarcoma cells, transduced the cells with either a GFP or an XBP1s-encoding adenovirus, and examined the N-glycosylation pattern on secreted CD2 under both conditions. We observe a strong enhancement of higher molecular weight N-glycoforms in cells where XBP1s is expressed (Figure 6D). Together, these data indicate that the striking impacts of XBP1s activation on N-glycan maturation are restricted neither just to the CD2 protein nor just to HEK293 cells.

DISCUSSION

Our results demonstrate the capacity of XBP1s-mediated remodeling of the ER proteostasis environment to enhance the biosynthesis of particular hybrid and complex N-glycans. Although it is not yet possible to conclusively attribute the observed alterations in N-glycan maturation to specific enzymes upregulated by XBP1s in Figure 1A, roles for the upregulation of GNT-I and MAN1A1 in the enhanced synthesis of hybrid N-glycans and the upregulation of GNT-II in the enhanced synthesis of complex N-glycans are plausible. We speculate that similar XBP1s-induced effects may apply more broadly across the endogenous N-glycoproteome. In ongoing work, we are performing N-glycoproteome-wide studies on endogenous proteins in the context of small molecule-mediated UPR activation to explore this possibility.

Considering the classical role of the UPR in resolving protein misfolding stress, there is the possibility that XBP1s-mediated changes in N-glycosylation patterns assist ER protein folding either indirectly by orchestrating interactions with ER proteostasis network components or directly by altering folding biophysics. Bearing in mind that the IRE1-XBP1s axis is the only arm of the UPR conserved across all eukaryotes (Walter and Ron, 2011), it is alternatively possible that XBP1s simply plays a critical role in regulating all aspects of ER client production. The effects observed need not be linked directly to resolving protein misfolding stress. In such a scenario, regulating N-glycan maturation is a previously unappreciated, yet nonetheless critical role of XBP1s.

There are diverse potential biological implications of XBP1s-mediated regulation of the molecular architecture of mature N-glycans. For example, specific N-glycan structures have roles in processes including protein sorting to microvesicles (Batista et al., 2011) and cell-cell recognition (Sharon, 2007) that would be influenced by altered N-glycan maturation. In addition, a number of secreted proteins displaying high-mannose N-glycoforms after Golgi processing are known (de Leoz et al., 2011; Satoh et al., 2007), so a specific shift away from high-mannose N-glycans upon XBP1s activation could influence protein recognition and uptake via the mannose receptor (East and Isacke, 2002). Altered N-glycosylation upon XBP1s activation could

also potentially play a role in transcellular communication of ER stress (Taylor and Dillin, 2013), an XBP1s-dependent and important biological process for which the relevant signaling molecule remains to be identified.

Of particular interest is the correlation between unusual N-glycoform populations in many cancers (Fry et al., 2011; Häuselmann and Borsig, 2014; Stowell et al., 2015) and constitutive activation of the IRE1-XBP1s UPR axis in certain malignancies (Bagratuni et al., 2010; Carrasco et al., 2007; Fujimoto et al., 2003). There is the possibility that XBP1s activity mechanistically links particular neoplastic N-glycosylation patterns to chronic ER protein misfolding stress in cancer. An XBP1s-induced shift toward hybrid and especially certain complex N-glycans could enhance tumor invasiveness (Stowell et al., 2015). Our data in Table 1 also suggest that XBP1s activation may increase sialylation. To date, three mechanisms have been proposed to induce hypersialylation in cancer (Büll et al., 2014); XBP1s activation may represent a fourth mechanism.

Aside from the intriguing biological implications of our findings, we also note that XBP1s activation has previously been employed to increase the yield of recombinant antibodies and other proteins (Tigges and Fussenegger, 2006). Our findings suggest that controlling XBP1s provides a valuable mechanism to modulate N-glycan biosynthesis on recombinant N-glycoproteins, particularly in cases where undesirable high-mannose N-glycans are abundantly produced.

SIGNIFICANCE

The cellular mechanisms that dynamically regulate the N-glycome remain poorly understood. Here, we leverage chemical biology tools for stress-independent, small molecule-mediated control of the UPR to discover that the UPR can regulate the molecular architecture of mature N-linked glycans via XBP1s-mediated remodeling of N-glycan biosynthesis pathways. Specifically, we show that XBP1s activation strongly enhances the synthesis of particular hybrid and complex N-glycans on model secreted proteins. Detailed glycomic analyses show that the identities of terminal N-glycan epitopes are also influenced by XBP1s activation. These effects cannot be attributed to altered secretion or degradation of particular N-glycoforms, indicating a genuine alteration of N-glycan maturation. Our results are significant because they provide a mechanistic link between intracellular stress responses classically involved in maintaining proteostasis and the molecular architecture of the extracellular N-glycome. There are numerous plausible biological consequences of this freshly drawn connection. In particular, it is well-established that many malignant cells display both unusual N-glycosylation patterns and constitutive XBP1s activation. There may be a causative relationship between these two observations, a possibility we are currently exploring. Also noteworthy, the trafficking of many proteins is influenced by their N-glycan structures, as are the strengths of interactions between N-glycoproteins and various lectins or cell surface proteins. Via these pathways, XBP1s-mediated effects on N-glycan architectures may play a functional role in processes ranging from cancer metastasis to auto-immunity. Furthermore, transcellular communication of stress signals plays an important role in organism survival in the face of stress, yet the signaling molecule has remained elusive. XBP1s-altered N-glycosylation patterns may play a role. Finally, improved methods are needed to optimize N-glycan architectures on recombinant proteins produced for biotechnology applications. Small molecule-mediated, stress-independent control of XBP1s signaling could prove useful for such a purpose.

EXPERIMENTAL PROCEDURES

Cell Culture, Plasmids, and Transfections

HEK293 cells were cultured in DMEM supplemented with glutamine, penicillin/streptomycin, 10% fetal bovine serum (FBS), and appropriate selection agents as previously described (Shoulders et al., 2013b). A stable HEK293$^{DAX\text{-}CD2}$ cell line constitutively expressing the CD2 adhesion domain from *R. norvegicus*, whose primary amino acid sequence is shown in the Supplemental Experimental Procedures, was created by transduction of HEK293^{DAX} cells with CD2-encoding lentivirus (Campeau et al., 2009) and maintained in 1.2 μg/ml puromycin after single colony selection. A stable HEK293^{DAX} cell line expressing the collagen-α1(I) C-propeptide was created by calcium phosphate-mediated co-transfection of the appropriate vector (vide infra) with a puromycin linear marker (ClonTech) and selection in 1.2 μg/ml puromycin. Saos-2 cells were cultured in complete DMEM supplemented with 15% heat-inactivated FBS. Transient transfections of eGFP-N3 or CD2.pFLAG-CMV3 were performed using polyethylenimine or X-tremeGENE 9 (Roche).

eGFP-N3 and CD2.pFLAG-CMV3 were generous gifts from Professor J.W. Kelly (Scripps Research Institute). For lentivirus production, the gene encoding CD2 was transferred to pENTR1A using the BamHI and NotI sites and then shuttled into pLenti.CMV.Puro DEST (Campeau et al., 2009) using LR clonase II-mediated recombination. The C-propeptide domain of *COL1A1* (residues 1,218–1,464) was PCR-amplified from a *COL1A1*-encoding vector and inserted into the pcDNA3.1 vector downstream of a 5′-preprotrypsin signal sequence followed by an HA epitope tag.

Immunoblotting and SDS-PAGE

Proteins were separated by SDS-PAGE using 12% Bis-Tris gels. Immunoblotting was performed as previously described (Shoulders et al., 2013b) and analyzed using a Li-Cor Biosciences Odyssey Imager. Antibodies employed are listed in the Supplemental Experimental Procedures.

Quantitative RT-PCR

The relative mRNA expression levels of target genes were measured using quantitative RT-PCR (see the Supplemental Experimental Procedures for details and Table S2 for a list of primers used).

[^{35}S] Metabolic Labeling Experiments

HEK293$^{DAX\text{-}CD2}$ cells seeded on poly-D-lysine-coated plates were treated with Dox at 1 μg/ml to activate XBP1s for 24 hr. Cells were then starved for 1 hr in DMEM + 10% FBS lacking Cys and Met. Cells were metabolically labeled in pulse medium containing [^{35}S]-Cys/Met (MP Biomedicals, ~0.1 mCi/ml final concentration) for 20 min, then incubated in pre-warmed chase media for the indicated times. Lactacystin (10 μM) was added as indicated at the beginning of the chase period. Medium was collected and cells were lysed in a 1% Triton X-100 buffer. CD2 was immunopurified using M2 anti-FLAG agarose beads (Sigma; A2220) and washed with radio-immunoprecipitation assay buffer. Immunoisolates were eluted by boiling in 6× Laemmli buffer and separated by SDS-PAGE. The gels were then dried, exposed to phosphorimager plates (GE Healthcare), and imaged with a Typhoon imager. Band intensities were quantified in ImageQuant TL.

Enzyme Digestions

PNGase F, Endo-H, Endo-F$_3$, α1–2,3-mannosidase, and α1–6-mannosidase were obtained from NEB. Digestions were performed according to the manufacturer's protocols.

MALDI-TOF MS/MS Glycomic Analyses

CD2 was purified upon secretion from untreated and XBP1s-activated HEK293$^{DAX\text{-}CD2}$ cells and purified CD2 SDS-gel bands were processed for N-glycan analysis as described in the Supplemental Experimental Procedures. MS and MS/MS data were acquired using a 4800 MALDI-TOF/TOF (Applied Biosystems) mass spectrometer. For MS/MS, the collision energy was set to 1 kV. Ar was used as the collision gas. The 4700 calibration standard kit, Calmix (Applied Biosystems), was used as the external calibrant for the MS mode of both instruments. Human [Glu1] fibrinopeptide B (Sigma) was used as an external calibrant for the MS/MS mode of the MALDI-TOF/TOF instrument. MS and MS/MS data were processed using Data Explorer 4.9 (Applied Biosystems) following the detailed protocol presented in the Supplemental Experimental Procedures.

SUPPLEMENTAL INFORMATION

Supplemental Information including Supplemental Experimental Procedures, two tables, and four figures can be found with this article online at http://dx.doi.org/10.1016/j.chembiol.2015.09.006.

ACKNOWLEDGMENTS

The authors gratefully acknowledge Pyae Hein, Amber Murray, and R. Luke Wiseman for helpful discussion. This work was supported by the 56th Edward Mallinckrodt Jr. Foundation Faculty Scholar Award, the NIH/NIAMS (1R03AR067503), a Mizutani Foundation for Glycoscience Innovation Grant, the Singapore-MIT Alliance for Research and Technology, and MIT (all to M.D.S.); by the Biotechnology and Biological Sciences Research Council Grant BB/K016164/1 (Core Support for Collaborative Research to A.D. and S.M.H.); and by the Wellcome Trust (Senior Investigator Award to A.D.). This work was also supported in part by the NIH/NIEHS (P30-ES002109). A.S.D. was supported by the NIH/NIAMS (F31AR067615).

Received: April 30, 2015
Revised: September 6, 2015
Accepted: September 9, 2015
Published: October 22, 2015

REFERENCES

Aebi, M. (2013). N-Linked protein glycosylation in the ER. Biochim. Biophys. Acta *1833*, 2430–2437.

Bagratuni, T., Wu, P., de Castro, D.G., Davenport, E.L., Dickens, N.J., Walker, B.A., Boyd, K., Johnson, D.C., Gregory, W., Morgan, G.J., et al. (2010). XBP1s levels are implicated in the biology and outcome of myeloma mediating different clinical outcomes to thalidomide-based treatments. Blood *116*, 250–253.

Batista, B.S., Eng, W.S., Pilobello, K.T., Hendricks-Muñoz, K.D., and Mahal, L.K. (2011). Identification of a conserved glycan signature for microvesicles. J. Proteome Res. *10*, 4624–4633.

Braakman, I., and Bulleid, N.J. (2011). Protein folding and modification in the mammalian endoplasmic reticulum. Annu. Rev. Biochem. *80*, 71–99.

Büll, C., Stoel, M.A., den Brok, M.H., and Adema, G.J. (2014). Sialic acids sweeten a tumor's life. Cancer Res. *74*, 3199–3204.

Campeau, E., Ruhl, V.E., Rodier, F., Smith, C.L., Rahmberg, B.L., Fuss, J.O., Campisi, J., Yaswen, P., Cooper, P.K., and Kaufman, P.D. (2009). A versatile viral system for expression and depletion of proteins in mammalian cells. PLoS One *4*, e6529.

Caramelo, J.J., and Parodi, A.J. (2008). Getting in and out from calnexin/calreticulin cycles. J. Biol. Chem. *283*, 10221–10225.

Carrasco, D.R., Sukhdeo, K., Protopopova, M., Sinha, R., Enos, M., Carrasco, D.E., Zheng, M., Mani, M., Henderson, J., Pinkus, G.S., et al. (2007). The differentiation and stress response factor XBP-1 drives multiple myeloma pathogenesis. Cancer Cell *11*, 349–360.

Ceroni, A., Maass, K., Geyer, H., Geyer, R., Dell, A., and Haslam, S.M. (2008). GlycoWorkbench: A tool for the computer-assisted annotation of mass spectra of glycans. J. Proteome Res. *7*, 1650–1659.

Chen, M.M., Bartlett, A.I., Nerenberg, P.S., Friel, C.T., Hackenberger, C.P.R., Stultz, C.M., Radford, S.E., and Imperiali, B. (2010). Perturbing the folding energy landscape of the bacterial immunity protein Im7 by site-specific N-linked glycosylation. Proc. Natl. Acad. Sci. USA *107*, 22528–22533.

Chui, D., Sellakumar, G., Green, R.S., Sutton-Smith, M., McQuistan, T., Marek, K.W., Morris, H., Dell, A., and Marth, J.D. (2001). Genetic remodeling of protein glycosylation in vivo induces autoimmune disease. Proc. Natl. Acad. Sci. USA *98*, 1142–1147.

Culyba, E.K., Price, J.L., Hanson, S.R., Dhar, A., Wong, C.-H., Gruebele, M., Powers, E.T., and Kelly, J.W. (2011). Protein native-state stabilization by placing aromatic side chains in N-glycosylated reverse turns. Science *331*, 571–575.

de Leoz, M.L.A., Young, L.J.T., An, H.J., Kronewitter, S.R., Kim, J., Miyamoto, S., Borowsky, A.D., Chew, H.K., and Lebrilla, C.B. (2011). High-mannose glycans are elevated during breast cancer progression. Mol. Cell. Proteomics *10*, M110.002717.

Dennis, J.W., Nabi, I.R., and Demetriou, M. (2009). Metabolism, cell surface organization, and disease. Cell *139*, 1229–1241.

Denzel, M.S., Storm, N.J., Gutschmidt, A., Baddi, R., Hinze, Y., Jarosch, E., Sommer, T., Hoppe, T., and Antebi, A. (2014). Hexosamine pathway metabolites enhance protein quality control and prolong life. Cell *156*, 1167–1178.

East, L., and Isacke, C.M. (2002). The mannose receptor family. Biochim. Biophys. Acta *1572*, 364–386.

Elbein, A.D., Tropea, J.E., Mitchell, M., and Kaushal, G.P. (1990). Kifunensine, a potent inhibitor of the glycoprotein processing mannosidase I. J. Biol. Chem. *265*, 15599–15605.

Elliott, S., Lorenzini, T., Asher, S., Aoki, K., Brankow, D., Buck, L., Busse, L., Chang, D., Fuller, J., Grant, J., et al. (2003). Enhancement of therapeutic protein in vivo activities through glycoengineering. Nat. Biotechnol. *21*, 414–421.

Fry, S.A., Afrough, B., Lomax-Browne, H.J., Timms, J.F., Velentzis, L.S., and Leathem, A.J.C. (2011). Lectin microarray profiling of metastatic breast cancers. Glycobiology *21*, 1060–1070.

Fujimoto, T., Onda, M., Nagai, H., Nagahata, T., Ogawa, K., and Emi, M. (2003). Upregulation and overexpression of human X-box binding protein 1 (hXBP-1) gene in primary breast cancers. Breast Cancer *10*, 301–306.

Hammond, C., Braakman, I., and Helenius, A. (1994). Role of N-linked oligosaccharide recognition, glucose trimming, and calnexin in glycoprotein folding and quality control. Proc. Natl. Acad. Sci. USA *91*, 913–917.

Hassinen, A., Pujol, F.M., Kokkonen, N., Pieters, C., Kihlström, M., Korhonen, K., and Kellokumpu, S. (2011). Functional organization of Golgi N- and O-glycosylation pathways involves pH-dependent complex formation that is impaired in cancer cells. J. Biol. Chem. *286*, 38329–38340.

Häuselmann, I., and Borsig, L. (2014). Altered tumor-cell glycosylation promotes metastasis. Front Oncol. *4*, 28.

Herscovics, A. (1999). Importance of glycosidases in mammalian glycoprotein biosynthesis. Biochim. Biophys. Acta *1473*, 96–107.

Ioannou, Y.A., Zeidner, K.M., Grace, M.E., and Desnick, R.J. (1998). Human α-galactosidase A: glycosylation site 3 is essential for enzyme solubility. Biochem. J. *332*, 789–797.

Iwamoto, M., Björklund, T., Lundberg, C., Kirik, D., and Wandless, T.J. (2010). A general chemical method to regulate protein stability in the mammalian central nervous system. Chem. Biol. *17*, 981–988.

Jacob, G.S., and Scudder, P. (1994). Glycosidases in structural analysis. Methods Enzymol. *230*, 280–299.

Jang-Lee, J., North, S.J., Sutton-Smith, M., Goldberg, D., Panico, M., Morris, H., Haslam, S., and Dell, A. (2006). Glycomic profiling of cells and tissues by mass spectrometry: Fingerprinting and sequencing methodologies. Methods Enzymol. *415*, 59–86.

Lau, K.S., Partridge, E.A., Grigorian, A., Silvescu, C.I., Reinhold, V.N., Demetriou, M., and Dennis, J.W. (2007). Complex N-glycan number and degree of branching cooperate to regulate cell proliferation and differentiation. Cell *129*, 123–134.

Lee, A.-H., Iwakoshi, N.N., and Glimcher, L.H. (2003). XBP-1 regulates a subset of endoplasmic reticulum resident chaperone genes in the unfolded protein response. Mol. Cell. Biol. *23*, 7448–7459.

Lehle, L., and Tanner, W. (1976). The specific site of tunicamycin inhibition in the formation of dolichol-bound N-acetylglucosamine derivatives. FEBS Lett. *71*, 167–170.

Moremen, K.W., Tiemeyer, M., and Nairn, A.V. (2012). Vertebrate protein glycosylation: diversity, synthesis and function. Nat. Rev. Mol. Cell Biol. *13*, 448–462.

Murray, A.N., Chen, W., Antonopoulos, A., Hanson, S.R., Wiseman, R.L., Dell, A., Haslam, S.M., Powers, D.L., Powers, E.T., and Kelly, J.W. (2015). Enhanced aromatic sequons increase oligosaccharyltransferase glycosylation efficiency and glycan homogeneity. Chem. Biol. *22*, 1052–1062.

Ron, D., and Walter, P. (2007). Signal integration in the endoplasmic reticulum unfolded protein response. Nat. Rev. Mol. Cell Biol. *8*, 519–529.

Ruiz-Canada, C., Kelleher, D.J., and Gilmore, R. (2009). Cotranslational and posttranslational N-glycosylation of polypeptides by distinct mammalian OST isoforms. Cell *136*, 272–283.

Satoh, T., Cowieson, N.P., Hakamata, W., Ideo, H., Fukushima, K., Kurihara, M., Kato, R., Yamashita, K., and Wakatsuki, S. (2007). Structural basis for recognition of high mannose type glycoproteins by mammalian transport lectin VIP36. J. Biol. Chem. *282*, 28246–28255.

Schröder, M., and Kaufman, R.J. (2005). The mammalian unfolded protein response. Annu. Rev. Biochem. *74*, 739–789.

Sharon, N. (2007). Lectins: Carbohydrate-specific reagents and biological recognition molecules. J. Biol. Chem. *282*, 2753–2764.

Shoulders, M.D., and Raines, R.T. (2009). Collagen structure and stability. Annu. Rev. Biochem. *78*, 929–958.

Shoulders, M.D., Ryno, L.M., Cooley, C.B., Kelly, J.W., and Wiseman, R.L. (2013a). Broadly applicable methodology for the rapid and dosable small molecule-mediated regulation of transcription factors in human cells. J. Am. Chem. Soc. *135*, 8129–8132.

Shoulders, M.D., Ryno, L.M., Genereux, J.C., Moresco, J.J., Tu, P.G., Wu, C., Yates, J.R., 3rd, Su, A.I., Kelly, J.W., and Wiseman, R.L. (2013b). Stress-independent activation of XBP1s and/or ATF6 reveals three functionally diverse ER proteostasis environments. Cell Rep. *3*, 1279–1292.

Spear, E.D., and Ng, D.T.W. (2005). Single, context-specific glycans can target misfolded glycoproteins for ER-associated degradation. J. Cell Biol *169*, 73–82.

Stowell, S.R., Ju, T., and Cummings, R.D. (2015). Protein glycosylation in cancer. Annu. Rev. Pathol. Mech. Dis. *10*, 473–510.

Taylor, R.C., and Dillin, A. (2013). XBP-1 is a cell-nonautonomous regulator of stress resistance and longevity. Cell *153*, 1435–1447.

Thibault, G., Ismail, N., and Ng, D.T.W. (2011). The unfolded protein response supports cellular robustness as a broad-spectrum compensatory pathway. Proc. Natl. Acad. Sci. USA *108*, 20597–20602.

Tigges, M., and Fussenegger, M. (2006). XBP1-based engineering of secretory capacity enhances the productivity of Chinese hamster ovary cells. Metab. Eng. *8*, 264–272.

Tulsiani, D.R.P., Harris, T.M., and Touster, O. (1982). Swainsonine inhibits the biosynthesis of complex glycoproteins by inhibition of Golgi mannosidase II. J. Biol. Chem. *257*, 7936–7939.

Venetz, D., Hess, C., Lin, C.-W., Aebi, M., and Neri, D. (2015). Glycosylation profiles determine extravasation and disease-targeting properties of armed antibodies. Proc. Natl. Acad. Sci. USA *112*, 2000–2005.

Voss, M., Künzel, U., Higel, F., Kuhn, P.-H., Colombo, A., Fukumori, A., Haug-Kröper, M., Klier, B., Grammer, G., Seidl, A., et al. (2014). Shedding of glycan-modifying enzymes by signal peptide peptidase-like 3 (SPPL3) regulates cellular N-glycosylation. EMBO J. *33*, 2890–2905.

Walter, P., and Ron, D. (2011). The unfolded protein response: From stress pathway to homeostatic regulation. Science *334*, 1081–1086.

Wang, Z.V., Deng, Y., Gao, N., Pedrozo, Z., Li, D.L., Morales, C.R., Criollo, A., Luo, X., Tan, W., Jiang, N., et al. (2014). Spliced X-box binding protein 1 couples the unfolded protein response to hexosamine biosynthetic pathway. Cell *156*, 1179–1192.

Wujek, P., Kida, E., Walus, M., Wisniewski, K.E., and Golabek, A.A. (2004). N-Glycosylation is crucial for folding, trafficking, and stability of human tripeptidyl-peptidase I. J. Biol. Chem. *279*, 12827–12839.

Zielinska, D.F., Gnad, F., Wiśniewski, J.R., and Mann, M. (2010). Precision mapping of an in vivo N-glycoproteome reveals rigid topological and sequence constraints. Cell *141*, 897–907.

